Science of the Total Environment 790 (2021) 147974

Contents lists available at ScienceDirect

Science of the Total Environment

journal homepage: www.elsevier.com/locate/scitotenv

Estimation of the biogeochemical reactivities of dissolved organic matter from modified biochars using color

Mingxing Wang [a], Jiang Liu [b], Luo Peng [a], Shanyi Tian [c], Caiyun Yang [d], Guomin Xu [e,f], Dingyong Wang [a], Tao Jiang [a,*]

[a] State Cultivation Base of Eco-Agriculture for Southwest Mountainous Land, Department of Environmental Sciences and Engineering, College of Resources and Environment, Southwest University, Chongqing 400716, China
[b] State Key Laboratory of Environmental Geochemistry, Institute of Geochemistry, Chinese Academy of Sciences, Guiyang 550002, China
[c] Soil Ecology Laboratory, College of Resources and Environmental Sciences, Nanjing Agricultural University, Nanjing 210095, China
[d] Research Center of Bioenergy and Bioremediation, College of Resources and Environment, Southwest University, Chongqing 400716, China
[e] National Engineering Research Center for Compounding and Modification of Polymer Materials, Guiyang 550014, China
[f] Guizhou Material Industrial Technology Institute, Guiyang 550014, China

HIGHLIGHTS

- Biochar-borne dissolved organic matter (DOM_{BC}) was extracted from biochar.
- The DOM_{BC} from modified biochar degrades faster and has a lower EDC.
- The aromaticity and molecular weight predominantly affect the DOM_{BC} properties.
- We propose a new method for DOM_{BC} analysis and biochar reactivity prediction.
- Our results indicate the advantages of optical analysis in the assessment of biochar.

GRAPHICAL ABSTRACT

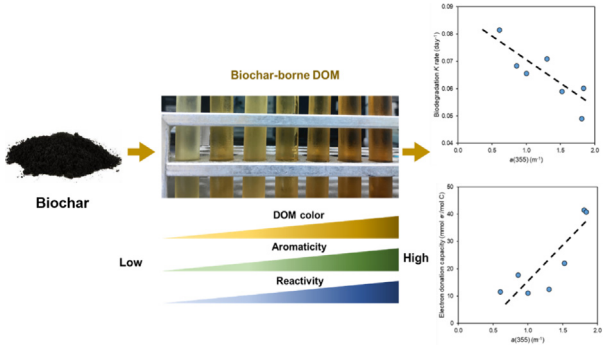

ARTICLE INFO

Article history:
Received 25 February 2021
Received in revised form 28 April 2021
Accepted 19 May 2021
Available online 25 May 2021

Editor: Baoliang Chen

Keywords:
Soil amendment
Aromaticity
Electron-donating capacity
Optical spectroscopy

ABSTRACT

Modified biochar is widely used as a soil amendment in agricultural systems to improve crop yields and remove environmental pollutants. The water-soluble fraction of biochar, called biochar-derived dissolved organic matter (DOM_{BC}), is the most active biochar component. However, the correlation between the optical properties of DOM_{BC} and its biogeochemical activity remain unclear. In this study, one biochar and six modified derivatives were used to extract DOM_{BC} and characterize its optical properties. The biogeochemical reactivities of DOM_{BC} were determined using biodegradation, photodegradation, and electron-donating capacity assays. The results show that modification changes the biochar characteristics, leading to a variety of DOM_{BC} properties. The DOM_{BC} from modified biochars degrades more rapidly than the original biochar. On the other hand, modification reduces the redox functional groups in DOM_{BC}, resulting in a lower electron-donating capacity of DOM samples. However, the modifications did not seem to affect photodegradation. Not all spectral parameters provide information about the correlations between the DOM_{BC} properties and biogeochemical reactivity. However, two fundamental properties, that is, the specific UV absorbance at 254 nm ($SUVA_{254}$, showing aromaticity) and spectral slopes over the ranges of 275–295 nm of the UV absorbance ($S_{275-295}$, showing molecular weight), are the dominant factors affecting the

* Corresponding author.
E-mail address: jiangtower666@163.com (T. Jiang).

https://doi.org/10.1016/j.scitotenv.2021.147974

Biodegradation
Photodegradation

biodegradation and electron-donating capacities of DOM_{BC}. In this study, a rapid and straightforward method is presented, which can be used to characterize DOM_{BC} and predict the reactivity of biochar that is used as an environmental amendment to minimize toxic organic compounds.

1. Introduction

Biochar (BC), which is an efficient and low-cost soil amendment, is produced from the pyrolysis of organic biomass under limited oxygen supply (Huang et al., 2019a; Li et al., 2018; Naeem et al., 2021; Zubair et al., 2021). Many biomass types, such as plants, grasses, municipal sludge, agricultural residue, manure, food waste, paper mill waste, and feedstock, can be used to produce biochar (Liu et al., 2015; Turan, 2019, 2020; Khan et al., 2020) via various thermochemical processes. Biochar is widely used in soil to ameliorate agricultural systems (Tang et al., 2019), enhance crop yield (Ahmad et al., 2014; Shahbaz et al., 2019), and mitigate greenhouse gas emissions (Das et al., 2021). Because of its various functional groups, biochar can also immobilize environmental contaminants, such as heavy metals, and thus reduce the toxicity and bioaccumulation risk in soils. In addition, biochar is one of the most used low-cost adsorbents for the removal of many types of pollutants from aqueous solutions (Ahmad et al., 2014; Tan et al., 2016a; Huang et al., 2019b).

In recent years, numerous studies have focused on biochar modification (i.e., engineered biochar) with the goal to form new structures and enhance surface properties (Yang and Jiang, 2014; Li et al., 2018). Modified biochars generally exhibit a significantly improved biogeochemical reactivity, which is due to the introduction of new functional groups and components (e.g., amino, chitosan, and sulfhydryl; Jin et al., 2017; Yang and Jiang, 2014). For example, catalytic material-integrated biochar plays a dual role as an adsorbent and catalytic degradation agent during the removal of organic contaminants (Han et al., 2015; Tan et al., 2016b). Yang and Jiang (2014) reported that amino acids enhance the ability of biochar to adsorb copper (Cu) from synthetic wastewater. In addition, chitosan-modified biochars has shown an enhanced heavy metal removal ability, especially for lead (Pb) (Zhou et al., 2013). Thiol-modified biochars are also highly efficient in the removal of mercury (Hg) and methylmercury (Huang et al., 2019b; Lyu et al., 2020). This type of biochar has also been used in the remediation of cadmium (Cd)- and Pb-polluted soils (Fan et al., 2020). Sulfur impregnation of biochar is an efficient way to enhance the Hg removal, which is due to the formation of HgS precipitates (Tan et al., 2016a).

The water-soluble fraction of biochar, called biochar-derived dissolved organic matter (DOM_{BC}), is released from bulk biochar when in contact with an aqueous phase. As the most active component of biochar, the structural and compositional characteristics of DOM_{BC} largely determine its applicability to soils. Similar to DOM identified in natural systems (e.g., lakes, forest soil, and rivers), DOM_{BC} plays an essential role in the carbon cycle, environmental fate of contaminants such as polycyclic aromatic hydrocarbons (Tang et al., 2016), mercury (Liu et al., 2019), and some organic wastes (Klammsteiner et al., 2020), and the responses of aquatic microorganisms to toxic material (Smith et al., 2016). For example, the aromatic moiety facilitates electron transfer, resulting in variations in the redox activity of DOM_{BC} (Graber et al., 2014). In addition, the biodegradability of DOM_{BC} is related to carbon sequestration, which could further influence the soil fertility and microbial activity (Mitchell et al., 2015). Thus, considering the wide application of biochar, the determination of the characteristics of DOM_{BC}, especially from bulk biochar, is essential to understand the role of biochar-derived DOM in soil systems.

Optical methods, including ultraviolet visible (UV–Vis) and fluorescence spectroscopy, have been widely applied to measure and characterize DOM in natural and engineered environments because of their high sensitivity, simplicity, rapid analysis, and in situ-measurements capabilities. The "fingerprint" of DOM, that is, the optical parameters, reflects specific characteristics of the water quality. For example, the specific UV absorbance at 254 nm ($SUVA_{254}$) is a classic optical parameter representing the DOM aromaticity (Weishaar et al., 2003; McKnight et al., 2001). This property is also used to evaluate the biogeochemical reactivity of DOM. In water treatment engineering, the optical parameters of DOM have been used to characterize the biological oxygen demand (BOD) removal efficiency and trace organic contaminant transformation of different treatment methods (Henderson et al., 2009; Korak et al., 2014; Carstea et al., 2016). However, a standard approach with respect to the selection of optical parameters for the evaluation of the DOM reactivities has not been established. Despite previous studies on the characterization of different types of DOM_{BC} (Li et al., 2018), the correlation between its characteristics and reactivity remains unclear. Therefore, it is necessary to validate whether an optical parameter can be used to evaluate the biogeochemical reactivity of DOM_{BC}.

Therefore, we hypothesized that the diverse DOM_{BC} characteristics control its biogeochemical reactivity. The aims of this study were (1) to characterize DOM_{BC} from modified biochars; (2) to elucidate the correlations between the DOM_{BC} properties and its biogeochemical reactivity; and (3) to determine if compositional parameters can be used as indicators of the reactivity of DOM_{BC}.

2. Materials and methods

2.1. Biochar and biochar-derived DOM

Original biochar ($BC_{original}$) was produced from pinecones, which were purchased from ShiKeJinNian Biotech Ltd. (Guizhou Bijie, China). Modified samples were obtained by chemically grafting different functional groups on the biochar, including amino (BC_{NH2}), epoxy ($BC_{CH(O)CH}$), ethyoxyl (BC_{C2H5O}), and thiol (BC_{thiol}) groups. Two biochars were chemically coated to introduce selenium (BC_{Se}) and chitosan ($BC_{chitosan}$). In this study, biochar-derived DOM (i.e., DOM_{BC}) samples were extracted using Milli-Q® water (18.2 Ω·cm) following a modified method of soil DOM extraction (Jiang et al., 2017; Wei et al., 2019, 2020). The biochar powder/water ratio was 1:100 g/mL. The powder suspension was maintained on a horizontal shaking device (220 rpm) at room temperature in the dark for 48 h. The suspension was then centrifuged for 30 min at 4000 rpm. Subsequently, 0.45 μm polyether sulfone (PES) membranes were used to filter the supernatant and collect the DOM_{BC}. The DOM samples were frozen and stored. Prior to the analyses, the DOM_{BC} samples were diluted 500 times (e.g., diluted samples).

2.2. DOM characterization

The DOM concentration, that is, the dissolved organic carbon (DOC; $mg \cdot L^{-1}$), was measured using a total organic carbon (TOC) analyzer (Shimadzu TOC-L, Japan). The UV–Vis and fluorescence measurements were conducted at room temperature in a 10 mm quartz cuvette using an Aqualog® (Horiba, Japan) absorption–fluorescence spectrometer equipped with a 150 W ozone-free xenon lamp. Milli-Q® water was used as a blank. The UV–Vis scan ranged from 230 to 800 nm at 1 nm intervals. The specific UV absorbance at 254 nm ($SUVA_{254}$, $L \cdot mg^{-1} \cdot m^{-1}$) was calculated as follows: $SUVA_{254} = A(254)/DOC$, where A(254) is the sample absorption absorbance at 254 nm after correcting for iron (Jaffrain et al., 2007; Weishaar et al., 2003). The Naperian absorption coefficient was calculated as $a(\lambda) = 2.303^{*}A/l$, where $a(\lambda)$ is the DOM absorption coefficients at wavelength λ (nm),

A is the absorbance, and l is the cuvette path length (m). We selected the absorption coefficient $a(355)$ to indicate the abundance of chromophoric DOM. Emission–excitation matrices (EEMs) were recorded using fluorescence spectroscopy. Corrections of the inner-filter effects (IFE) were described in our previous study (Jiang et al., 2018). In particular, parallel absorbance measurement from the sample and blank (Milli-Q water) was conducted (Yang and Hur, 2014) and Aqualog® EEMS data processing software was used to correct the IFE automatically. In addition, corrections for the IFE were double-checked using OriginPro 2017. The emission spectra ranged from 250 to 620 nm at 3.18 nm steps and the excitation spectra ranged from 230 to 450 nm at 5 nm. The fluorescence index (FI) was calculated as the ratio of the fluorescence intensities at emission wavelengths of 470 and 520 nm (excitation wavelength was maintained at 370 nm; McKnight et al., 2001; Fellman et al., 2010; Cory and McKnight, 2005). The biological index (BIX) was calculated by dividing the emission intensity at 380 nm by the emission intensity of the maximum value in the range of 420–435 nm at an excitation of 310 nm (Huguet et al., 2009; Wilson and Xenopoulos, 2009). In addition, the humification index (HIX) was calculated by dividing the peak area under the emission spectra at 435–480 nm by 300–445 nm at a constant excitation of 254 nm (Zsolnay et al., 1999; Ohno et al., 2007; Huguet et al., 2009).

2.3. Biochemical reactivities assay

2.3.1. Biodegrading reactivity

The biodegradation kinetics experiment was carried out on a multi-connected magnetic stirring system (NB-9, Suzhou Jiulian Technology, Suzhou, China) at room temperature. Subsequently, 250 mL diluted biochar-DOM samples were added into brown reaction bottles and inoculated with 30 mL bacterial solution (InterLab Polyseed ®, USA). A stirrer (250 rpm) was placed in each reaction bottle and the total degradation period was 5 d. Biodegraded solutions were subsampled after 0, 1, 2, 3, and 5 d of incubation. Subsequently, all collected samples were filtered through 0.22 μm PES membranes and stored at 4 °C in the dark before performing spectral analyses. InterLab Polyseed® bacterial inoculum was purchased from Hach® Company (catalog 29187-00, USA). Detailed information is provided in the Supporting Information. The biodegradation rate was calculated using the following pseudo-first-order equation: $DOC_t/DOC_0 = \exp.(-k \times t)$, where DOC_t is the residual DOC at a certain time (t), DOC_0 is the initial DOC, and k (d^{-1}) is the kinetic rate constant. The biodegradation degree (%) was obtained as follows: $(DOC_0 - DOC_t) \times 100/DOC_0$. Three replicates were used for the experiment.

2.3.2. Electrochemical evaluation of the electron-donating capacity

Mediated electrochemical oxidation (MEO) analysis was conducted to determine the electron-donating capacity (EDC) of DOM_{BC}. The three-electrode system consisted of a carbon felt working electrode (1 cm × 1 cm × 0.3 cm), Ag/AgCl (saturated) reference electrode, and Pt wire counter electrode. The electrochemical cell had a volume of 8 mL and accommodated an electrolyte consisting of 0.1 M KCl and 0.1 M phosphate buffer. During the measurements, the working electrode was poised at 0.61 V, whereas the electrolyte was continuously stirred using a magnetic bar (150 rpm). After the start of the chronoamperometry, the reactor was supplemented with 0.1 mL of 2,2′-azino-bis (3-ethylbenzothiazoline-6-sulfonic acid solution (ABTS, 10 mM; Macklin®, Shanghai China). The samples (0.1 mL) were then sequentially injected into the reactor. Each injection took place after the current spike (due to the previous injection) stabilized. The charge transfer was calculated by integrating each current peak. The EDC of DOM, also called reducing capacity (RC), was normalized and reported in mmol e^-/mol carbon unit.

2.3.3. Photodegradation reactivity

The photodegradation experiment was conducted at room temperature using an RLH-18 photoreaction system (Beijing Nuozhi Technology, Beijing, China) with a 3 W LED light source. The stock biochar DOM was placed in a photodegradation test tube. The chromophoric DOM, also called colored DOM (CDOM) [i.e., $a(355)$] was used as an indicator to monitor the photodegradation kinetics. The DOM samples were collected on days 0, 1, 3, 5, and 7. All samples were stored at 4 °C in the dark before spectral analysis. The photodegradation rate was calculated using a pseudo-first-order equation: $CDOM_t/CDOM_0 = \exp.(-k \times t)$, where $CDOM_0$ is the initial CDOM, $CDOM_t$ is the residual CDOM after photodegradation for a certain time (t), and k (d^{-1}) is the kinetic rate constant. The degree of the degradation (%) was obtained as follows: $(CDOM_0 - CDOM_t) \times 100/CDOM_0$.

2.4. Data analysis

All statistical analyses were conducted using OriginPro® 2017, Microsoft® Excel, and SPSS 23. The Lilliefors test was used to confirm the normality of all datasets. The dataset differences were assessed with a t-test with a significance level of 0.05 ($p < 0.05$). Linear correlations between the parameters of the different methods were assessed using Pearson's r_p coefficients.

3. Results and discussion

3.1. Biochar-derived DOM characteristics

Regarding the water/biochar mass ratio (i.e., for the extraction of the water-soluble organic C fraction), the DOC concentrations of the original (298.50 $mg \cdot L^{-1}$) and modified (mean 437.36 ± 94.96 $mg \cdot L^{-1}$) biochars differed. Higher DOC concentrations were detected in the modified biochars ($p < 0.01$). This may be attributed to the different pyrolytic conditions used for modification. Similar differences have been reported for the DOM release from biochar, which were explained by the differences in the original biomasses and pyrolytic temperatures (Tang et al., 2016). The CDOM abundance is represented by the decadic absorptivity $a(355)$ (Jiang et al., 2020a, 2020b). To avoid the inner filter effect (IFE), after 500 dilutions of DOM extracted at the same solid/water ratio (i.e., 1:100 g/mL), the $a(355)$ ranged from 0.60 to 1.84 m^{-1}. When the CDOM was normalized to DOC (CDOM/DOC, $L \cdot mg^{-1} \cdot m^{-1}$), we observed a decrease in the modified DOM_{BC}. After the modification, the variable coefficient (VC, %) of fluorophores and chromophores and optical index of DOM_{BC} varied from 5.1% (i.e., FI index) to 62.6% (i.e., $a(355)$/DOC). These large variations suggest that the compositions of the samples significantly changed due to the modification, although the DOM_{BC} of modified biochars was derived from the same bulk biochar.

Five fluorescence peaks are observed in the EEMs based on "peak-picking" (Coble, 1996, 2007; Coble et al., 2014; Birdwell and Engel, 2009), that is, humic-like A (Ex/Em = 250–260 nm/380–480 nm) and C (Ex/Em = 330–350 nm/420–480 nm), tyrosine-like peak B (Ex/Em = 270–280 nm/300–320 nm), and tryptophan-like T (Ex/Em = 270–280 nm/320–350 nm) peaks, as shown in Fig. S1 in the Supporting Information. Moreover, the ultraviolet A (UVA) humic-like component is generally called M peak, which is located at (Ex/Em = 290–325 nm/370–430 nm). Peak M is considered to represent a pool of microbially processed humic-like materials. These peaks have been widely reported for DOM samples from natural water, soil, and sediments, suggesting both autochthonous and allochthonous sources (Fellman et al., 2010; Hansen et al., 2016). Similar fluorescent components were also observed in other studies of biochar extracts from birch and maple (Jamieson et al., 2014), agricultural residues and sludge (Tang et al., 2016), and DOM derived from amended soils (Smebye et al., 2016).

Previous studies showed that the biogeochemical reactivity of DOM is related to its aromaticity, as defined by indicators, such as $SUVA_{254}$, which is widely used as a proxy for the aromaticity of natural organic matter (NOM) (Weishaar et al., 2003; McKnight et al., 2001; Spencer et al., 2012). After modification, DOM_{BC} showed a notably lower $SUVA_{254}$ ($p = 0.001$, with one exception of BC_{Se}) and higher $S_{275–295}$

than the original biochar ($p < 0.001$). We also calculated the aromaticity of DOM_{BC} based on the linear relationship between $SUVA_{254}$ (by UV–Vis) and the aromaticity (by ^{13}C NMR) using the following equation (Walpen et al., 2016): $SUVA_{254} = 0.115 \times$ aromatic C (%) + 1.4. The average estimated aromaticity of all samples was 14% and of the modified and original biochar-derived DOM was 12% and 26%, respectively. This suggests that the modification introduced new functional groups to the original bulk but destroyed the DOM structure. The changes in both indices indicate the loss of aromatic moieties and decrease in the molecular weight of DOM_{BC}. It has been previously reported that $S_{275–295}$ negatively correlates with the hydrophobic DOM fraction, suggesting the high aromaticity of DOM with high molecular weight (Helms et al., 2008; Spencer et al., 2012; Jiang et al., 2017). However, we did not observe such a correlation between $SUVA_{254}$ and higher $S_{275–295}$ values ($r_p = -0.64$, $p = 0.12$) in this study (Fig. 1a). This decoupling may be explained by the fact that changes in the molecular weight of DOM might not be merely attributed to changes in the aromaticity.

The FI values of all samples range from 1.4 to 1.9, suggesting a combination of autochthonous and allochthonous sources. It is noted that the end members of FI (i.e., defined at 1.4 and 1.9) originated from natural organic matter (McKnight et al., 2001), which suggests that differences may occur when applying these values to biochar-derived DOM. Similar FI values can be found in DOM extracted from biochar prepared from different materials (Table S1). The BIX shows a good linear correlation with the FI (Fig. 1b), suggesting fluorophores with structures similar to autochthonous DOM may exist in biochar-derived DOM. In contrast to the UV–Vis indices, the modification of the DOM_{BC} fluorescence properties is minimal because the differences among BIX, HIX, and FI are insignificant. However, the normalized fluorescence peaks and CDOM (i.e., fluorescence peaks and CDOM normalized by DOC) significantly differed ($p < 0.01$). It is worth noting that CDOM, that is, $a(355)$, significantly positively correlates with $SUVA_{254}$ ($r_p = 0.85$, $p = 0.02$; Fig. 1c) and negatively correlates with $S_{275–295}$ ($r_p = -0.86$, $p = 0.01$; Fig. 1c). This suggests that the chromophore fractions of DOM_{BC} are mainly dominated by aromatic moieties with high molecular weights, especially fulvic-like components, as reflected by the fluorescence peak A, based on the significant correlation between peak A and $SUVA_{254}$ (Fig. 1d).

3.2. Biodegradation assay of DOM_{BC}

Fig. 2a shows the kinetic changes in the DOC concentrations during the five-day incubation period. The pseudo-first-order equation adequately describes the biodegradation kinetics of DOM_{BC}. The average kinetic rate is $0.065 \pm 0.010\ d^{-1}$. After the modification, the degradation rate of biochar-derived DOM increases (average $0.068 \pm 0.008\ d^{-1}$) compared with that of the original sample ($0.049\ d^{-1}$), which results in a higher degree of biodegradation (average 30.6% ± 4.4%) at the end of this assay (Fig. 2b). In addition, the half-life of DOM_{BC} derived from modified biochars is also shorter (average ~ 10.9 d) than that of the original DOM_{BC} (~14.1 d).

The UV–Vis parameters provide information about the fluorescence properties of DOM_{BC}, which poorly reflect the correlation between the DOM structure and reactivity. The results of this study show that the CDOM, CDOM normalized with DOC (i.e., CDOM/DOC), and $S_{275–295}$ significantly correlate with the biodegradation rate [i.e., k (d^{-1}); Fig. 3a–c]. This suggests that the chromophores and molecular weight of the DOM are both key factors affecting biodegradability. The relationship between the k constant and $S_{275–295}$ (Fig. 3a, $r_p = 0.85$, $p = 0.02$) indicates that fractions with low molecular weights, such as simple sugars, amino

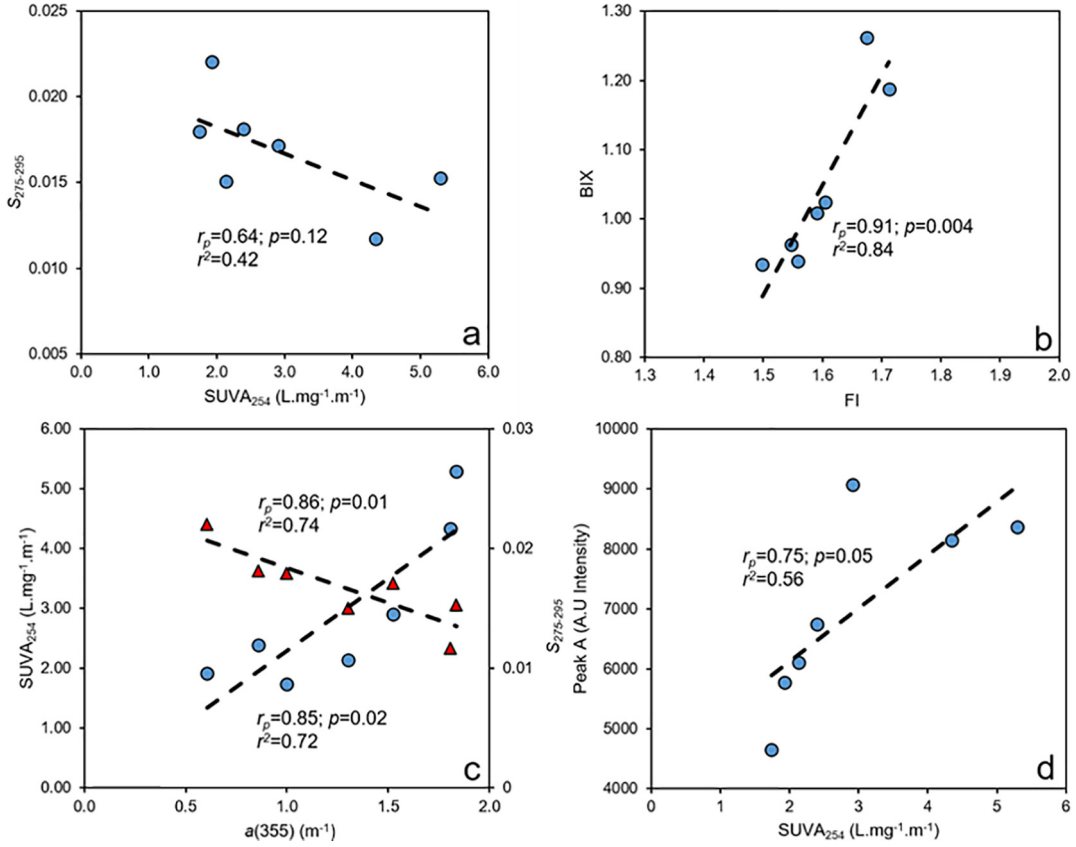

Fig. 1. Correlations between (a) specific UV absorbance ($SUVA_{254}$) and spectral slope ($S_{275–295}$), (b) fluorescence and biological indices (FI and BIX, respectively), (c) $SUVA_{254}$ and $S_{275–295}$ and chromophoric dissolved organic matter (CDOM), (d) and $SUVA_{254}$ and fluorescent peak A for biochar-derived DOM ($n = 7$). The light green and brown shadow regions in (b) represent autochthonous and allochthonous origins, respectively. The red triangles and blue circles in plot (c) indicate the correlations between $SUVA_{254}$ and CDOM and $S_{275–295}$ and CDOM, respectively. Black dashed lines represent the linear regressions. (For interpretation of the references to color in this figure legend, the reader is referred to the web version of this article.)

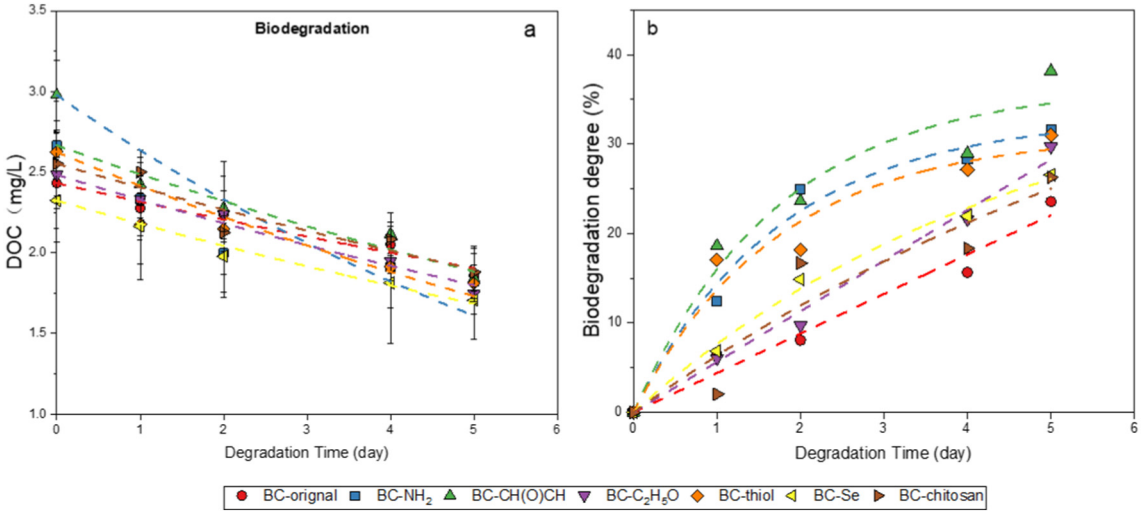

Fig. 2. Kinetic processes of biodegradation of biochar-derived dissolved organic matter (DOM), including (a) dissolved organic carbon (DOC) changes and (b) biodegradation degree (%). Different color dash lines represent the fitting curve by pseudo-first-order rate law.

acids, and aliphatic acids, are more biodegradable. The most common approach to determine the bioreactivity of DOM is a biodegradation assay based on bottle incubation experiments, which better reflects the labile fractions (Shen and Benner, 2020). Given the 5-day incubation period, the kinetic rate demonstrates that the DOM from modified biochars is more labile.

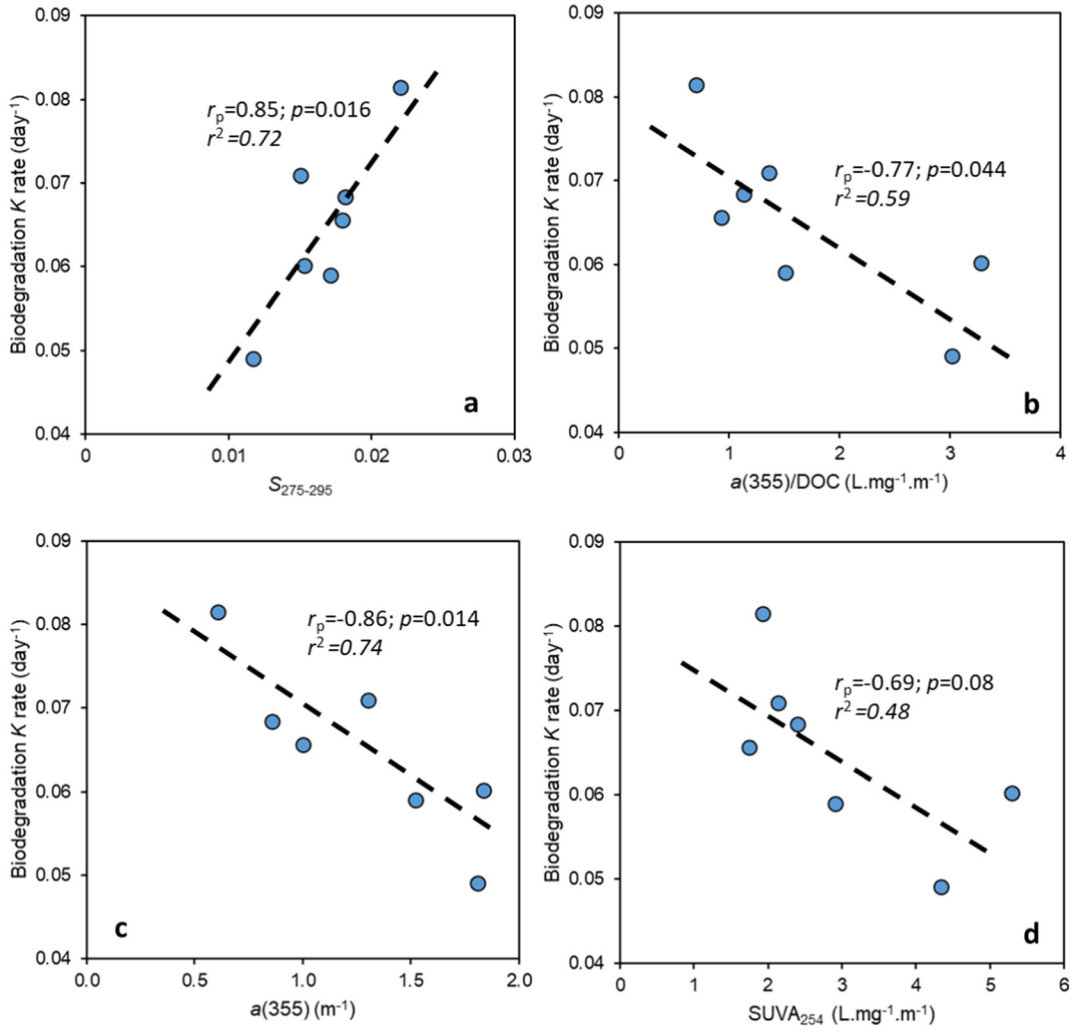

Fig. 3. Correlations between the biodegradation kinetic rate (d^{-1}) and (a) $S_{275-295}$, (b) CDOM/DOC, (c) CDOM, and (d) $SUVA_{254}$ ($n = 7$). The black dashed lines represent the linear regressions.

The results of the present study show that $SUVA_{254}$ and the biodegradability rate of DOM_{BC} are not correlated significantly ($r_p = -0.69$, $p = 0.08$; Fig. 3d). However, this negative correlation suggests that the aromatic component is less labile, thus decelerating the degradation rate compared with labile components such as proteins and sugars. Based on the results of this study, DOM from modified biochars with a higher biodegradation rate may be a potential but labile organic matter pool in terrestrial or aquatic systems. Therefore, it could play a role as a priming substrate and substantially influence the carbon cycle, especially in soils (Blagodatskaya and Kuzyakov, 2008; Bianchi, 2011).

3.3. Electron donation capacities of DOM_{BC}

The redox reactivity of DOM in the environment is generally described in terms of its ability to shuttle electrons. The ability to transfer electrons facilitates the reduction of many major/trace elements and pollutants such as iron (Fe; Kappler et al., 2004; Peretyazhko and Sposito, 2006; Piepenbrock et al., 2014; Royer et al., 2002), arsenic (As; Zhang et al., 2020a), chromium (Cr; Gu and Chen, 2003; Maurer et al., 2012), copper (Cu; Pham et al., 2012; Maurer et al., 2013), and mercury (Hg; Gu et al., 2011; Jiang et al., 2015, 2020a, 2020b). Thus, understanding the redox properties of biochar-derived DOM, especially the electron donation, is crucial for predicting its role in environmental biogeochemical redox reactions. Based on the MEO method, the EDC range was 11.1–46.1 mmol e^-/mol C. Considering the small pH differences of DOM_{BC} (6.9–7.6), the effect of the pH on the EDC can be excluded. Fig. 4a shows the correlation between the EDC of all samples and $SUVA_{254}$. The EDC increases with increasing $SUVA_{254}$. This indicates that the aromaticity, including phenols and quinones, is a major redox-active moiety in DOM_{BC}. Compared with the original sample, the modified biochar-derived DOM samples exhibit significantly lower EDC values ($p < 0.01$), which implied that the DOM derived from biochar without modification has a higher potential to reduce heavy metals. This suggests that the modification decreases the number of redox functional groups such as quinones. Considering the EDC values normalized by the corresponding $SUVA_{254}$ values, to account for variations in DOM aromaticity among samples, the larger EDC from the original DOM_{BC} became more apparent. After the normalization by $SUVA_{254}$, the $EDC_{normalization}$ values of the original DOM_{BC} (0.80 μmol $e^- \cdot m \cdot L^{-1}$) were still higher than those of the modified samples (0.60 μmol $e^- \cdot m \cdot L^{-1}$). Thus, the lower $EDC_{normalization}$ values observed in the modified DOM_{BC} indicate the removal of phenols during the modification. Similar reductions in the EDC per unit aromaticity (i.e., $EDC/SUVA_{254}$) were also reported for "older" and more processed terrestrial DOM and explained by the depletion of phenolic moieties (Aeschbacher et al., 2012).

The CDOM [i.e., a (355)] and CDOM/DOC [i.e., a(355)/DOC] also demonstrate the effect of the abundance of chromophoric constituents in DOM on the observed EDC (Fig. 4b and c). More chromophores in DOM may imply higher unsaturation with redox moieties, contributing to a greater EDC. This is not surprising because aromatic structures, that is, the hosts of redox functional groups, are generally the main components of light absorbance spectra of DOM (Fig. 1c).

In addition, fluorescent peaks A and T significantly correlate with RC (Fig. 4d and e). The correlations are stronger yet not significant compared with those with peaks B ($p = 0.06$), M ($p = 0.10$), and C ($p = 0.07$; Fig. S3). This suggests that fulvic- and tryptophan-like components dominantly control the EDC. This further indicates that phenolic moieties of humic- and protein-like components contribute to the EDC. This is not surprising regarding the effects of protein-like components on the EDC. Jiang et al. (2020a) used pyrolysis to determine the protein components that positively affect the reducing capacities of soil DOM of the kinetic rate of inorganic Hg(II) reduction. In addition, other DOM samples with heavy microbial fingerprints showed significant reducing capacities such as DOM from composts (He et al., 2019; Xiao et al., 2019) and a typical autochthonous lake in the Antarctic (Aeschbacher et al., 2012). Compared with humic-like components, which involve direct electron transfer due to aromatic structures, protein-like components may affect the steric availability of redox moieties and thus the final kinetic rate. It is noted that soils amended with original biochar would be more sensitive to redox changes compared with those amended with modified biochar. Thus, it should be carefully applied as an amendment in redox-dynamic areas such as rice-paddy fields or water-level fluctuation zones of streams.

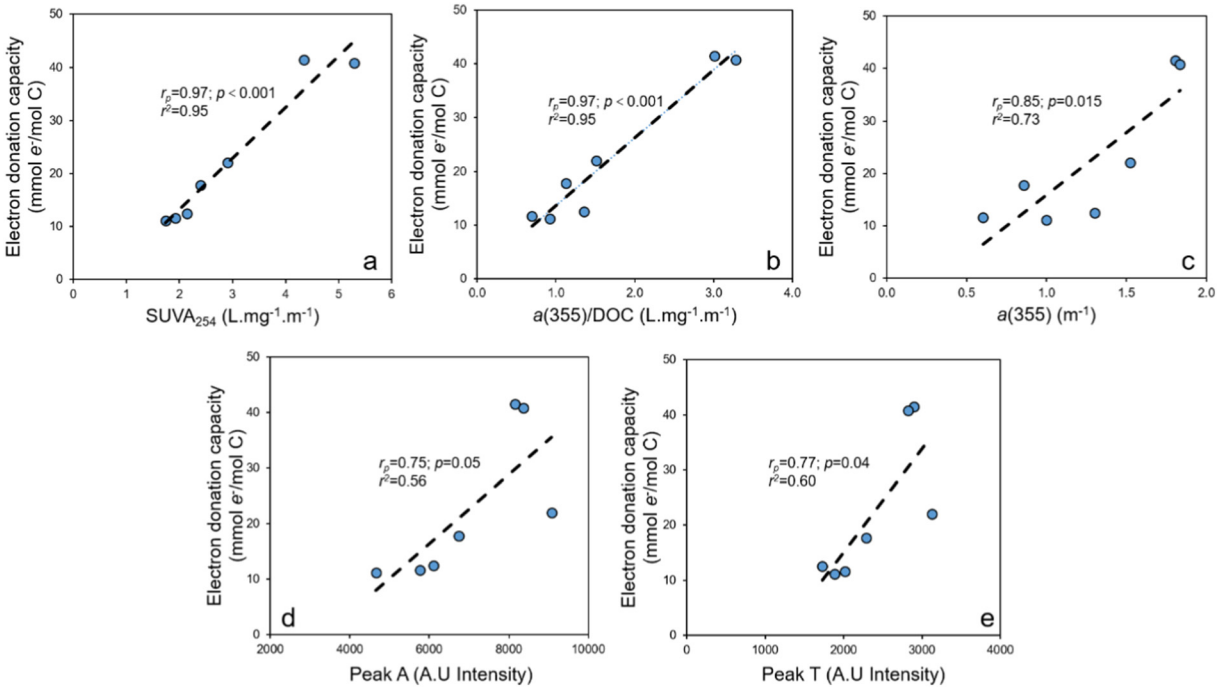

Fig. 4. Correlations between the electron donation capacity (mmol e^-/mol C) and (a) $SUVA_{254}$, (b) CDOM/DOC, (c) CDOM, (d) fluorescent peak A, and (e) fluorescent peak T ($n = 7$). The black dashed lines represent the linear regressions.

3.4. Photodegradation assay of DOM_{BC}

Photodegradation is a vital transformation process of DOM in aquatic environments (Page et al., 2013; Berg et al., 2019). In this study, the loss of CDOM [i.e., $a(355)$] was used for the quantification of the DOM decay with increasing photo-irradiation time (Fig. 5). After the 7-day photodegradation, 41%–52% of the DOC in all samples was photodegraded (mean of 48% ± 4%), except for DOM_{BC} from $BC_{CH(O)CH}$. The average kinetic rate (d^{-1}) was 0.10 ± 0.02, but the DOM_{BC} from $BC_{CH(O)CH}$ showed the slowest rate of 0.05 d^{-1}. After the modification, the DOM_{BC} concentration was slightly lower than that of the original sample, but the difference was insignificant. This suggests that the modification did not notably affect the photoreactivity of DOM_{BC}, in contrast to its biodegradability and EDC, that is, the photo-reactivity is independent of modification. In particular, the critical photochemically produced reactive intermediate (PPRI) ·OH significantly positively correlates with the EDC (Page et al., 2013; Berg et al., 2019). Thus, the EDC plays a crucial role in the photodegradation of DOM. However, this coupling relationship is not observed in our study (Fig. S4).

The photochemical reactivity of DOM_{BC} has been investigated in previous studies (Fu et al., 2016; Fang et al., 2017; Ward et al., 2014). The results showed that the aromaticity and molecular weight of DOM_{BC} might be responsible for the higher photoreactivity of DOM_{BC} compared with natural aquatic organic matter (Page et al., 2013; Du et al., 2019; Li et al., 2019; Zhang et al., 2020b). In addition, Berg et al. (2019) reported a linear correlation between the optical properties and quantum yields of triplet DOM (Φ_{3DOM}). The quantum yields of ·OH ($\Phi_{\cdot OH}$) decreased with increasing $SUVA_{254}$. However, we did not observe a significant correlation between the DOM_{BC} properties and its photochemical reactivity. Although CDOM and $SUVA_{254}$ notably correlate with the biodegradation and EDC reactivities, the aromaticity can only explain ~10% of the photodegradation degree (%) and kinetic rate (Fig. S5).

The variations in the DOM_{BC} characteristics but similar photodegradation potentials might suggest that the composition and structure of DOM_{BC} are highly heterogeneous and responsible for the decoupling observed in the photodegradation assay. However, neither the UV–Vis nor fluorescence analyses identified the individual molecules in these samples. The photochemical degradation of DOM is associated with the aromatic and chromophoric carbon contents and closely related to photochemical degradation pathways and quantum yields (Page et al., 2013; Berg et al., 2019). Therefore, more experiments are needed to describe the degradation mechanism in detail.

3.5. Comparison and limits

Currently, biochar is widely used as a soil amendment. The DOM-derived biochar plays a crucial role in controlling the efficiency of the biochar application. Although it has been shown that optical methods are useful for the assessment of the quality of DOM derived from biochar (Jamieson et al., 2014; Li et al., 2017; Zhang et al., 2020a; Song et al., 2020), correlations between the optical parameters and reactivities of DOM have only been analyzed in few studies (Tang et al., 2016). For example, the $SUVA_{254}$ of DOM_{BC} from soybean strow, rice straw, peanut, and mushroom residue positively correlates with the binding affinity of polycyclic aromatic hydrocarbon (PAH; Tang et al., 2016). This index was also used to track the changes in the aromaticity of DOM_{BC} during biodegradation (Huang et al., 2019a). However, no general models or typical parameters, except for $SUVA_{254}$, explicitly describe the "structure–reactivity" relationship. Previous reports (Liu et al., 2015; Li et al., 2017; Song et al., 2020) suggested that the high structural heterogeneity of DOM_{BC} due to pyrolysis temperature, biomass, or application rate, could affect the DOM_{BC} characteristics. Therefore, the aromaticity and molecular weight are the dominant factors determining the variations in the biogeochemical reactivities of DOM_{BC}.

However, not all spectral parameters used in this study provide information about the reactivities of DOM_{BC}. In contrast to UV–Vis measurements, only the fluorescence peaks were sensitive to variations in the DOM_{BC} biogeochemical reactivity in this study. Fluorescent parameters, such as the FI, BIX, and HIX, did not show any correlations. For example, the BIX was expected to correlate with the bioavailability of DOM, but this correlation could not be confirmed. This might be explained by the structural complexity of the DOM, resulting in discrepancies in several optical parameters (Hansen et al., 2016; Jiang et al., 2017; Lescord et al., 2018). This was initially observed by Wagner et al. (2015) who used Fourier transform ion cyclotron resonance mass spectrometry (FT-ICR-MS) and reported that the FI shares some molecular families with $SUVA_{254}$, but maintains a close association with BIX, as we observed in this study. As validated by FT-ICR-MS, UV–Vis measurements are useful for the assessment of the DOM structure and composition and are rapid and cost-effective alternatives to high-resolution instruments such as FT-ICR-MS or orbitrap-MS (Maizel et al., 2017; Kellerman et al., 2018).

4. Conclusion

Biochar-derived DOM from the same original but modified material exhibits different optical properties, resulting in various biogeochemical

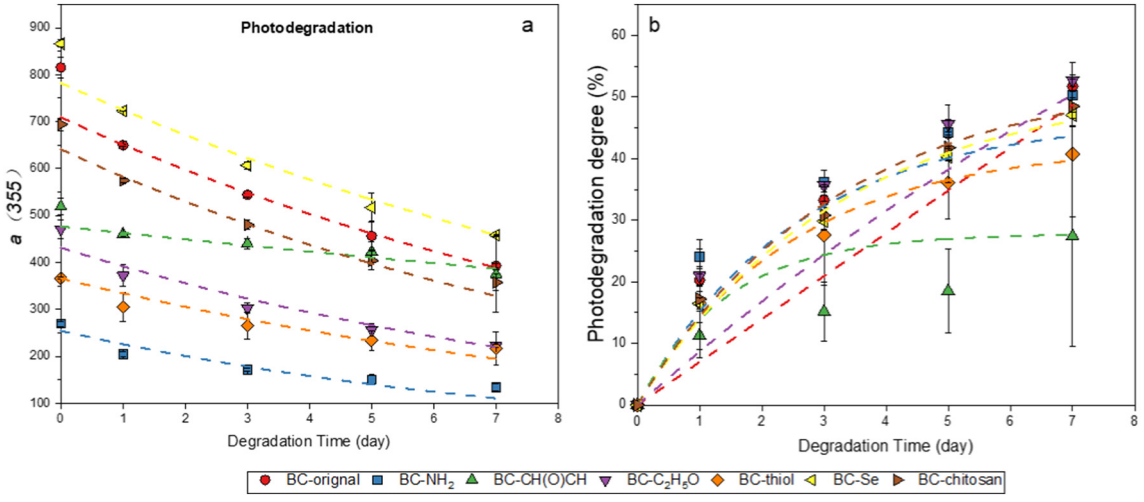

Fig. 5. Kinetic photodegradation processes of biochar-derived DOM including (a) CDOM changes and (b) the photodegradation degree (%). Different color dash lines represent the fitting curve by pseudo-first-order rate law.

reactivities, except for photodegradation. Chromophoric components of DOM_{BC} are the main factors affecting its reactivity with respect to biodegradation and EDC. In contrast to fluorophores, chromophores provide useful information for the evaluation of the DOM reactivity. In essence, the correlation between the DOM color and its biogeochemical reactivity is due to the dominance of the aromaticity. It should be emphasized that the samples analyzed in this study originated from the same parent biochar (i.e., original biochar). Therefore, the results, especially the CDOM, cannot be extrapolated to a more generalized DOM horizon, that is, samples with different origins. However, although the optical parameters are specific to DOM_{BC}, the framework of this study can be adapted to other scenarios. We also highlight the utility of simple optical measurements for the assessment of the reactivities of biochar-derived DOM. Optical analysis may provide valuable information regarding the characteristics of biochar-derived DOM and thus further assess its use as an environmental amendment for the minimization and remediation of toxic organic compounds.

CRediT authorship contribution statement

Mingxing Wang: Methodology, Software, Investigation, Data Curation, Formal analysis, and Writing-Original draft preparation

Jiang Liu: Methodology, Software, Investigation, Data Curation, Formal analysis, and Writing-Original draft preparation

Luo Peng: Methodology in electrochemical analysis, Data Curation, Formal analysis, Discussion, and Writing-Original draft preparation

Shanyi Tian: Investigation, Data Curation, Formal analysis, and Writing-Original draft preparation

Caiyun Yang: Discussion, Writing-Original draft preparation, and Writing-reviewing and editing

Guomin Xu: Experimental materials prepare and develop, Formal analysis, and Discussion

Dingyong Wang: Project Supervision; Conceptualization, Methodology, Formal analysis, and Writing-reviewing and editing

Tao Jiang: Project Supervision; Conceptualization, Methodology, Investigation, Formal analysis, Writing-reviewing, and editing

Declaration of competing interest

The authors declare that they have no known competing financial interests or personal relationships that could have appeared to influence the work reported in this paper.

Acknowledgments

This research was financially supported by the National Natural Science Foundation of China (NSFC) (41977275). Dr. Tao Jiang personally appreciates the open funding (PTS2020-01) from Hubei Key Laboratory of Environmental and Health Effects of Persistent Toxic Substances in Institute of Environment and Health, Jianghan University. He also would like to thank the State Key Laboratory of Environmental Chemistry and Ecotoxicology (SKLECE) of Research Center for Eco-Environmental Sciences, Chinese Academy of Science (CAS), for the generous support of the open grant (KF2020-08). Additionally, the Science and Technology Support Plan Project of Guizhou Province (2019-2836) was appreciated for its support.

Appendix A. Supplementary data

Supplementary data to this article can be found online at https://doi.org/10.1016/j.scitotenv.2021.147974.

References

Aeschbacher, M., Graf, C., Schwarzenbach, R.P., Sander, M., 2012. Antioxidant properties of humic substances. Environ. Sci. Technol. 46, 4916–4925.

Ahmad, M., Rajapaksha, A.U., Lim, J.E., Zhang, M., Bolan, N., Mohan, D., Vithanage, M., Lee, S.S., Ok, Y.S., 2014. Biochar as a sorbent for contaminant management in soil and water: a review. Chemosphere 99, 19–33.

Berg, S.M., Whiting, Q.T., Herrli, J.A., Winkels, R., Wammer, K.H., Remucal, C.K., 2019. The role of dissolved organic matter composition in determining photochemical reactivity at the molecular level. Environ. Sci. Technol. 53, 11725–11734.

Bianchi, T.S., 2011. The role of terrestrially derived organic carbon in the coastal ocean: a changing paradigm and the priming effect. Proc. Natl. Acad. Sci. U. S. A. 108, 19473–19481.

Birdwell, J.E., Engel, A.S., 2009. Variability in terrestrial and microbial contributions to dissolved organic matter fluorescence in the Edwards aquifer, Central Texas. J. Cave Karst Stud. 71 (2), 144–156.

Blagodatskaya, E., Kuzyakov, Y., 2008. Mechanisms of real and apparent priming effects and their dependence on soil microbial biomass and community structure: critical review. Biol. Fertil. Soils 45, 115–131.

Carstea, E.M., Bridgeman, J., Baker, A., Reynolds, D.M., 2016. Fluorescence spectroscopy for wastewater monitoring: a review. Water Res. 95, 205–219.

Coble, P.G., 1996. Characterization of marine and terrestrial DOM in seawater using excitation–emission matrix spectroscopy. Mar. Chem. 51, 325–346.

Coble, P.G., 2007. Marine optical biogeochemistry: the chemistry of ocean color. Chem. Rev. 107 (2), 402–418.

Coble, P.G., Spencer, R.G.M., Baker, A., Reynolds, D.M., 2014. Aquatic organic matter fluorescence. In: Coble, P.G., Lead, J., Baker, A., Reynolds, D.M., Spencer, R.G.M. (Eds.), Aquatic Organic Matter Fluorescence. Cambridge University Press. US, pp. 75–122.

Cory, R.M., McKnight, D.M., 2005. Fluorescence spectroscopy reveals ubiquitous presence of oxidized and reduced quinones in DOM. Environ. Sci. Technol. 39, 8142–8149.

Das, S.K., Ghosh, G.K., Avasthe, R., 2021. Applications of biomass derived biochar in modern science and technology. Environ. Technol. Innov. 21, 101306.

Du, Z.Y., He, Y.S., Fan, J.N., Fu, H.Y., Zheng, S.R., Xu, Z.Y., Qu, X.L., Kong, A., Zhu, D.Q., 2019. Predicting apparent singlet oxygen quantum yields of dissolved black carbon and humic substances using spectroscopic indices. Chemosphere 194, 405–413.

Fan, J.J., Cai, C., Chi, H.F., Reid, B.J., Coulon, F., Zhang, Y.C., Hou, Y.W., 2020. Remediation of cadmium and lead polluted soil using thiol–modified biochar. J. Hazard. Mater. 388, 122037.

Fang, G.D., Liu, C., Wang, Y.J., Dionysiou, D.D., Zhou, D.M., 2017. Photogeneration of reactive oxygen species from biochar suspension for diethyl phthalate degradation. Appl. Catal. B Environ. 214, 34–45.

Fellman, J.B., Hood, E., Spencer, R.G.M., 2010. Fluorescence spectroscopy opens new windows into dissolved organic matter dynamics in freshwater ecosystems: a review. Limnol. Oceanogr. 55, 2452–2462.

Fu, H.Y., Liu, H.T., Mao, J.D., Chu, W.Y., Li, Q.L., Alvarez, P.J.J., Qu, X.L., Zhu, D.Q., 2016. Photochemistry of dissolved black carbon released from biochar: reactive oxygen species generation and phototransformation. Environ. Sci. Technol. 50, 1218–1226.

Graber, E.R., Tsechansky, L., Lew, B., Cohen, E., 2014. Reducing capacity of water extracts of biochars and their solubilization of soil Mn and Fe. Eur. J. Soil Sci. 65, 162–172.

Gu, B., Bian, Y., Miller, C.L., Dong, W., Jiang, X., Liang, L., 2011. Mercury reduction and complexation by natural organic matter in anoxic environments. Proc. Natl. Acad. Sci. U. S. A. 108 (4), 1479–1483.

Gu, B.H., Chen, J., 2003. Enhanced microbial reduction of Cr(VI) and U(VI) by different natural organic matter fractions. Geochim. Cosmochim. Acta 67 (19), 3575–3582.

Han, L., Xue, S., Zhao, S.C., Yan, J.C., Qian, L.B., Chen, M.F., 2015. Biochar supported nanoscale iron particles for the efficient removal of methyl orange dye in aqueous solutions. PLoS One 10 (7), e0132067.

Hansen, A.M., Kraus, T.E.C., Pellerin, B.A., Fleck, J.A., Downing, B.D., Bergamaschi, B.A., 2016. Optical properties of dissolved organic matter (DOM): effects of biological and photolytic degradation. Limnol. Oceanogr. 61 (3), 1015–1032.

He, X.S., Yang, C., You, S.H., Zhang, H., Xi, B.D., Yu, M.D., Liu, S.J., 2019. Redox properties of compost–derived organic matter and their association with polarity and molecular weight. Sci. Total Environ. 665 (15), 920–928.

Helms, J.R., Stubbins, A., Ritchie, J.D., Minor, E.C., Kieber, D.J., Mopper, K., 2008. Absorption spectral slopes and slope ratios as indicators of molecular weight, source, and photobleaching of chromophoric dissolved organic matter. Limnol. Oceanogr. 53 (3), 955–969.

Henderson, R.K., Baker, A., Murphy, K.R., Hambly, A., Stuetz, R.M., Khan, S.J., 2009. Fluorescence as a potential monitoring tool for recycled water systems: a review. Water Res. 43, 863–881.

Huang, M., Li, Z.W., Luo, N.L., Yang, R., Wen, J.J., Huang, B., Zeng, G.M., 2019a. Application potential of biochar in environment: insight from degradation of biochar–derived DOM and complexation of DOM with heavy metals. Sci. Total Environ. 646, 220–228.

Huang, Y., Xia, S., Lyu, J., Tang, J., 2019b. Highly efficient removal of aqueous Hg^{2+} and CH_3Hg^+ by selective modification of biochar with 3–mercaptopropyltrimethoxysilane. Chem. Eng. J. 360, 1646–1655.

Huguet, A., Vacher, L., Relexans, S., Saubusse, S., Froidefond, J.M., Parlanti, E., 2009. Properties of fluorescent dissolved organic matter in the Gironde estuary. Org. Geochem. 40 (6), 709–719.

Jaffrain, J., Gérard, F., Meyer, M., Ranger, J., 2007. Assessing the quality of dissolved organic matter in forest soils using ultraviolet absorption spectrophotometry. Soil Sci. Soc. Am. J. 71, 1851–1858.

Jamieson, T., Sager, E., Guéguen, C., 2014. Characterization of biochar–derived dissolved organic matter using UV–visible absorption and excitation–emission fluorescence spectroscopies. Chemosphere 103, 197–204.

Jiang, T., Skyllberg, U., Wei, S.Q., Wang, D.Y., Lu, S., Jiang, Z.M., Flanagan, D.C., 2015. Modeling of the structure–specific kinetics of abiotic, dark reduction of Hg(II) complexed by O/N and S functional groups in humic acids while accounting for time–dependent structural rearrangement. Geochim. Cosmochim. Acta 154, 151–167.

Jiang, T., Kaal, J., Liang, J., Zhang, Y.J., Wei, S.Q., Wang, D.Y., Green, N.W., 2017. Composition of dissolved organic matter (DOM) from periodically submerged soils in the three gorges reservoir areas as determined by elemental and optical analysis, infrared spectroscopy, pyrolysis–GC–MS and thermally assisted hydrolysis and methylation. Sci. Total Environ. 603–604, 461–471.
Jiang, T., Bravo, A.G., Skyllberg, U., Björn, E., Wang, D., Yan, H., Green, N.W., 2018. Influence of dissolved organic matter (DOM) characteristics on dissolved mercury (Hg) species composition in sediment porewater of lakes from southwest China. Water Res. 146, 146–158.
Jiang, T., Kaal, J., Liu, J., Liang, J., Zhang, Y.J., Wang, D.Y., 2020a. Linking the electron donation capacity to the molecular composition of soil dissolved organic matter from the Three Gorges Reservoir areas, China. J. Environ. Sci. 90, 146–156.
Jiang, T., Wang, D.Y., Meng, B., Chi, J.S., Laudon, H., Liu, J., 2020b. The concentrations and characteristics of dissolved organic matter in high–latitude lakes determine its ambient reducing capacity. Water Res. 169, 115217.
Jin, J., Sun, K., Wang, Z.Y., Yang, Y., Han, L.F., Xing, B.X., 2017. Characterization and phenanthrene sorption of natural and pyrogenic organic matter fractions. Environ. Sci. Technol. 51 (5), 2635–2642.
Kappler, A., Benz, M., Schink, B., Brune, A., 2004. Electron shuttling via humic acids in microbial iron(III) reduction in a freshwater sediment. FEMS Microbiol. Ecol. 47, 85–92.
Kellerman, A.M., Guillemette, F., Podgorski, D.C., Aiken, G.R., Butler, K.D., Spencer, R.G.M., 2018. Unifying concepts linking dissolved organic matter composition to persistence in aquatic ecosystems. Environ. Sci. Technol. 52 (5), 2538–2548.
Khan, M.A., Mahmood-ur-Rahman, Ramzani, P.M.A., Zubair, M., Rasool, B., Khan, M.K., Ahmed, A., Khan, S.A., Turan, V., Iqbal, M., 2020. Associative effects of lignin–derived biochar and arbuscular mycorrhizal fungi applied to soil polluted from Pb–acid batteries effluents on barley grain safety. Sci. Total Environ. 710, 136294.
Klammsteiner, T., Turan, V., Juárez, M.F.D., Oberegger, S., Insam, H., 2020. Suitability of black soldier fly frass as soil amendment and implication for organic waste hygienization. Agronomy 10, 1578.
Korak, J.A., Dotson, A.D., Summers, R.S., Rosario-Ortiz, F.L., 2014. Critical analysis of commonly used fluorescence metrices to characterize dissolved organic matter. Water Res. 49, 327–338.
Lescord, G.L., Emilson, E.J.S., Johnston, T.A., Branfireun, B.A., Gunn, J.M., 2018. Optical properties of dissolved organic matter and their relation to mercury concentrations in water and biota across a remote freshwater drainage basin. Environ. Sci. Technol. 52, 3344–3353.
Li, M., Zhang, A., Wu, H., Liu, H., Lv, J., 2017. Predicting potential release of dissolved organic matter from biochars derived from agricultural residues using fluorescence and ultraviolet absorbance. J. Hazard. Mater. 334, 86–92.
Li, G., Khan, S., Ibrahim, M., Sun, T.-R., Tang, J.-F., Cotner, J.B., Xu, Y.-Y., 2018. Biochars induced modification of dissolved organic matter (DOM) in soil and its impact on mobility and bioaccumulation of arsenic and cadmium. J. Hazard. Mater. 348, 100–108.
Li, M., Bao, F.X., Zhang, Y., Sheng, H., Chen, C.C., Zhao, J.C., 2019. Photochemical aging of soot in the aqueous phase: release of dissolved black carbon and the formation of $^1O_2$. Environ. Sci. Technol. 53, 12311–12319.
Liu, P., Ptacek, C.J., Blowes, D.W., Berti, W.R., Landis, R.C., 2015. Aqueous leaching of organic acids and dissolved organic carbon from various biochars prepared at different temperatures. J. Environ. Qual. 44 (2), 684–695.
Liu, P., Ptacek, C.J., Blowes, D.W., 2019. Mercury complexation with dissolved organic matter released from thirty–six types of biochar. Bull. Environ. Contam. Toxicol. 103, 175–180.
Lyu, H.H., Xia, S.Y., Tang, J.C., Zhang, Y., Gao, B., Shen, B.X., 2020. Thiol–modified biochar synthesized by a facile ball–milling method for enhanced sorption of inorganic Hg^{2+} and organic CH_3Hg^+. J. Hazard. Mater. 384, 121357.
Maizel, A.C., Li, J., Remucal, C.K., 2017. Relationships between dissolved organic matter composition and photochemistry in lakes of diverse trophic status. Environ. Sci. Technol. 51, 9624–9632.
Maurer, F., Christl, I., Hoffmann, M., Kretzschmar, R., 2012. Reduction and reoxidation of humic acid: influence on speciation of cadmium and silver. Environ. Sci. Technol. 46, 8808–8816.
Maurer, F., Christl, I., Fulda, B., Voegelin, A., Kretzschmar, R., 2013. Copper redox transformation and complexation by reduced and oxidized soil humic acid. 2. Potentiometric titrations and dialysis cell experiments. Environ. Sci. Technol. 47, 10912–10921.
McKnight, D.M., Boyer, E.W., Westerhoff, P.K., Doran, P.T., Kulbe, T., Andersen, D.T., 2001. Spectrofluorometric characterization of dissolved organic matter for indication of precursor organic material and aromaticity. Limnol. Oceanogr. 46, 38–48.
Mitchell, P.J., Simpson, A.J., Soong, R., Simpson, M.J., 2015. Shifts in microbial community and water–extractable organic matter composition with biochar amendment in a temperate forest soil. Soil Biol. Biochem. 81, 244–254.
Naeem, I., Masood, N., Turan, V., Iqbal, M., 2021. Prospective usage of magnesium potassium phosphate cement combined with Bougainvillea alba derived biochar to reduce Pb bioavailability in soil and its uptake by Spinacia oleracea L. Ecotoxicol. Environ. Saf. 208, 111723.
Ohno, T., Fernandez, I.J., Hiradate, S., Sherman, J.F., 2007. Effects of soil acidification and forest type on water soluble organic matter properties. Geoderma 140, 176–187.
Page, S.E., Kling, G.W., Sander, M., Harrold, K.H., Logan, J.R., McNeill, K., Cory, R.M., 2013. Dark formation of hydroxyl radical in Arctic soil and surface waters. Environ. Sci. Technol. 47, 12860–12867.
Peretyazhko, T., Sposito, G., 2006. Reducing capacity of terrestrial humic acids. Geoderma 137, 140–146.
Pham, A.N., Rose, A.L., Waite, T.D., 2012. Kinetics of Cu(II) reduction by natural organic matter. J. Phys. Chem. A 116 (25), 6590–6599.
Piepenbrock, A., Schröder, C., Kappler, A., 2014. Electron transfer from humic substances to biogenic and abiogenic Fe(III) oxyhydroxide minerals. Environ. Sci. Technol. 48 (3), 1656–1664.
Royer, R.A., Burgos, W.D., Fisher, A.S., Jeon, B.H., Unz, R.F., Dempsey, B.A., 2002. Enhancement of hematite bioreduction by natural organic matter. Environ. Sci. Technol. 36 (13), 2897–2904.
Shahbaz, A.K., Adnan Ramzani, P.M., Saeed, R., Turan, V., Iqbal, Muhammad, Lewińska, K., Abbas, F., Saqib, M., Tauqeer, H.M., Iqbal, Mutahar, Fatima, M., Rahman, M. ur, 2019. Effects of biochar and zeolite soil amendments with foliar proline spray on nickel immobilization, nutritional quality and nickel concentrations in wheat. Ecotoxicol. Environ. Saf. 173, 182–191.
Shen, Y., Benner, R., 2020. Molecular properties are a primary control on the microbial utilization of dissolved organic matter in the ocean. Limnol. Oceanogr. 65 (5), 1061–1071.
Smebye, A., Alling, V., Vogt, R.D., Gadmar, T.C., Mulder, J., Cornelissen, G., Hale, S.E., 2016. Biochar amendment to soil changes dissolved organic matter content. Chemopshere 142, 100–105.
Smith, C.R., Hatcher, P.G., Kumar, S., Lee, J.W., 2016. Investigation into the sources of biochar water–soluble organic compounds and their potential toxicity on aquatic microorganisms. ACS Sustain. Chem. Eng. 4, 2550–2558.
Song, C.F., Shan, S.D., Yang, C., Zhang, C., Zhou, X.Q., Ma, Q., Yrjälä, K., Zheng, H.B., Cao, Y.C., 2020. The comparison of dissolved organic matter in hydrochars and biochars from pig manure. Sci. Total Environ. 72, 137423.
Spencer, R.G.M., Butler, K.D., Aiken, G.R., 2012. Dissolved organic carbon and chromophoric dissolved organic matter properties of rivers in the USA. J. Geophys. Res. Biogeosci. 117 (G3), G03001.
Tan, G.C., Sun, W.L., Xu, Y.R., Wang, H.Y., Xu, N., 2016a. Sorption of mercury (II) and atrazine by biochar, modified biochars and biochar based activated carbon in aqueous solution. Bioresour. Technol. 211, 727–735.
Tan, X.F., Liu, Y.G., Gu, Y.L., Xu, Y., Zeng, G.M., Hu, X.J., Liu, S.B., Wang, X., Liu, S.M., Li, L.J., 2016b. Biochar–based nano–composites for the decontamination of wastewater: a review. Bioresour. Technol. 212, 318–333.
Tang, F., Xu, Z., Gao, M., Li, L., Li, H., Cheng, H., Zhang, C., Tian, G., 2019. The dissipation of cyazofamid and its main metabolite in soil response oppositely to biochar application. Chemosphere 218, 26–35.
Tang, J.F., Li, X.H., Luo, Y., Li, G., Khan, S., 2016. Spectroscopic characterization of dissolved organic matter derived from different biochars and their polycylic aromatic hydrocarbons (PAHs) binding affinity. Chemosphere 152, 399–406.
Turan, V., 2019. Confident performance of chitosan and pistachio shell biochar on reducing Ni bioavailability in soil and plant plus improved the soil enzymatic activities, antioxidant defense system and nutritional quality of lettuce. Ecotoxicol. Environ. Saf. 183, 109594.
Turan, V., 2020. Potential of pistachio shell biochar and dicalcium phosphate combination to reduce Pb speciation in spinach, improved soil enzymatic activities, plant nutritional quality, and antioxidant defense system. Chemosphere 245, 125611.
Wagner, S., Jaffé, R., Cawley, K., Dittmar, T., Stubbins, A., 2015. Associations between the molecular and optical properties of dissolved organic matter in the Florida Everglades, a model coastal wetland system. Front. Chem. 3 (66), 66.
Walpen, N., Schroth, M.H., Sander, M., 2016. Quantification of phenolic antioxidant moieties in dissolved organic matter by flow–injection analysis with electrochemical detection. Environ. Sci. Technol. 50 (12), 6423–6432.
Ward, C.P., Sleighter, R.L., Hatcher, P.G., Cory, R.M., 2014. Insights into the complete and partial photooxidation of black carbon in surface waters. Environ Sci Process Impacts 16, 721–731.
Wei, J., Tu, C., Yuan, G.D., Bi, D.X., Wang, H.L., Zhang, L.J., Theng, B.K.J., 2019. Pyrolysis temperature–dependent changes in the characteristics of biochar–borne dissolved organic matter and its copper binding properties. Bull. Environ. Contam. Toxicol. 103 (1), 169–174.
Wei, J., Tu, C., Yuan, G.D., Zhou, Y.Q., Wang, H.L., Lu, J., 2020. Limited Cu(II) binding to biochar DOM: evidence from C K–edge NEXAFS and EEM–PARAFAC combined with two–dimensional correlation analysis. Sci. Total Environ. 701, 134919.1–134919.10.
Weishaar, J.L., Aiken, G.R., Bergamaschi, B.A., Fram, M.S., Fujii, R., Mopper, K., 2003. Evaluation of specific ultraviolet absorbance as an indicator of the chemical composition and reactivity of dissolved organic carbon. Environ. Sci. Technol. 37, 4702–4708.
Wilson, H.F., Xenopoulos, M.A., 2009. Effects of agricultural land use on the composition of fluvial dissolved organic matter. Nat. Geosci. 2, 37–41.
Xiao, X., Xi, B.D., He, X.S., Zhang, H., Li, D., Zhao, X.Y., Zhang, X.H., 2019. Hydrophobicity–dependent electron transfer capacities of dissolved organic matter derived from chicken manure compost. Chemosphere 222, 757–765.
Yang, G.X., Jiang, H., 2014. Amino modification of biochar for enhanced adsorption of copper ions from synthetic wastewater. Water Res. 48, 396–405.
Yang, L., Hur, J., 2014. Critical evaluation of spectroscopic indices for organic matter source tracing via end member mixing analysis based on two contrasting sources. Water Res. 59, 80–89.
Zhang, H., Shao, J.G., Zhang, S.H., Zhang, X., Chen, H.P., 2020a. Effect of phosphorus–modified biochars on immobilization of Cu (II), Cd (II), and As (V) in paddy soil. J. Hazard. Mater. 390, 121349.
Zhang, P., Shao, Y.F., Xu, X.J., Huang, P., Sun, H.W., 2020b. Phototransformation of biochar–derived dissolved organic matter and the effects on photodegradation of imidacloprid in aqueous solution under ultraviolet light. Sci. Total Environ. 724, 137913.
Zhou, Y., Gao, B., Zimmerman, A.R., Fang, J., Sun, Y., Cao, X., 2013. Sorption of heavy metals on chitosan–modified biochars and its biological effects. Chem. Eng. J. 231, 512–518.
Zsolnay, A., Baigar, E., Jimenez, M., Steinweg, B., Saccomandi, F., 1999. Differentiating with fluorescence spectroscopy the sources of dissolved organic matter in soils subjected to drying. Chemosphere 38, 45–50.
Zubair, M., Adnan Ramzani, P.M., Rasool, B., Khan, M.A., ur–Rahman, M., Akhtar, I., Turan, V., Tauqeer, H.M., Farhad, M., Khan, S.A., Iqbal, J., Iqbal, M., 2021. Efficacy of chitosan–coated textile waste biochar applied to Cd–polluted soil for reducing Cd mobility in soil and its distribution in moringa (Moringa oleifera L.). J. Environ. Manag. 284, 112047.